Biochemical and Biophysical Research Communications **268,** 148–154 (2000)
doi:10.1006/bbrc.2000.2090, available online at http://www.idealibrary.com on IDEAL®

Involvement of Intracellular Labile Zinc in Suppression of DEVD-Caspase Activity in Human Neuroblastoma Cells

Lien H. Ho, Ranjit N. Ratnaike, and Peter D. Zalewski[1]
Department of Medicine, University of Adelaide, Queen Elizabeth Hospital, Woodville, South Australia 5011, Australia

Received January 4, 2000

Age-related tissue Zn deficiency may contribute to neuronal and glial cell death by apoptosis in Alzheimer's dementia. To investigate this, we studied the effects of increasing or decreasing the levels of intracellular labile Zn on apoptosis of human neuroblastoma BE(2)-C cells *in vitro*. BE(2)-C cells were primed for 18 h with butyrate (1 mM) before addition of staurosporine (1 μM), an effector enzyme of apoptosis, for a further 3 h to induce DEVD-caspase activity. An increase in intracellular Zn using Zn ionophore pyrithione suppressed DEVD-caspase activity, while a decrease in intracellular Zn induced by Zn chelator TPEN mimicked staurosporine by activating DEVD-caspase in butyrate-primed cells. The distribution of intracellular Zn in the cells was demonstrated with the UV-excitable Zn-specific fluorophore Zinquin. Confocal images showed distinct cytoplasmic and cytoskeletal fluorescence. We propose that Zn decreases the level of apoptosis in neuronal cells exposed to toxins, possibly by stabilizing their cytoskeleton. © 2000 Academic Press

Alzheimer's disease (AD) and other dementias afflict a significant proportion of the elderly and place a heavy financial burden on health care systems. One area of the cell biology of AD of current interest is the cell suicide mechanism of apoptosis, which results in the loss of neurons and glial cells. For example, in AD, cell death in the hippocampus is increased up to 30-fold [1, 2]. Apoptosis is a normal mechanism, that serves to delete unwanted or moderately damaged cells, and is an important factor in determining normal tissue homeostasis and tumour growth and regression [3]. The apoptotic cell undergoes a series of morphological changes including decrease in cell volume, dramatic condensation of the chromatin, while maintaining membrane integrity. This eventually leads to the cell fragmenting into apoptotic bodies, which are then shed or phagocytosed.

Previous studies from our laboratory and others, both *in vitro* and *in vivo* [4, 5, and Refs. within], indicated a role for Zn in protection against premature apoptosis. Significant concentrations of Zn exist in the hippocampus and parts of the cerebral cortex, as a relatively free or loosely bound (labile) pool, and is important for memory function, cognition and behavior. These functions are affected in moderate Zn deficiency [6–8]. Different neuronal pools of Zn may serve different cellular functions, including nucleic acid synthesis [7], neurotransmitter storage and secretion in certain presynaptic terminals [8] and microtubule polymerization [9].

The influence of Zn on apoptosis has been well documented. Zn inhibits a Ca^{2+}- and Mg^{2+}-dependent endonuclease, resulting in the inhibition of DNA fragmentation, deemed as a late step of apoptosis [4]. Zn supplementation both *in vitro* and *in vivo* models have confirmed this inhibition. More recent studies have indicated a protective role for Zn in the earlier phases of apoptosis, especially the activation of the caspase family of proteases [10]. Principle amongst these is caspase-3 (formerly known as CPP-32), which in studies with gene-knockout mice has been shown to be important in controlling cell numbers in the brain [11]. Activation of caspase-3 involves the proteolytic processing of the 32-kDa cytosolic proenzyme to a tetrameric heterodimer of 17-kDa subunits and can be quantified by capacity of cell cytosol to cleave the fluorogenic substrate DEVD-AFC [12]. Perry and colleagues [13] have shown that Zn inhibits caspase-3 activity but only at millimolar concentrations of Zn. More recently, micromolar concentrations of Zn were shown to preferentially suppress caspase-6/Mch-2a, a caspase involved in lamin cleavage and activation caspase-3 [10, 14].

To study the effects of Zn on caspase-3 activation and apoptosis in neuronal cells, we have modified the model

Abbreviations used: AD, Alzheimer's disease; PBS, phosphate-buffered saline; zDEVD-AFC, z-asp-glu-val-asp-7-amino-4-trifluoromethyl-coumarin; $[Zn^{2+}]_i$, intracellular labile Zn concentration.

[1] To whom correspondence should be addressed. Fax: (+61) 8 8222 6042. E-mail: pzalewski@medicine.adelaide.edu.au.

0006-291X/00 $35.00

of Nuydens *et al.* [15]. They described a cellular model of AD in which human neuroblastoma cells are induced by the short chain fatty acid butyrate, to undergo essential protein synthesis leading to cytoskeletal alterations and apoptotic death. Butyrate induces aberrant gene expression by inhibition of histone deacetylase, resulting in hyperacetylation of histone H4, leading to the relaxation of the chromatin structure and increase in the availability of promoter elements of genes to transcription factors [16]. Butyrate, at low concentrations does not induce caspase-3 and apoptosis, but renders these cells highly susceptible to a second agent like the broad-spectrum protein kinase inhibitor staurosporine. Staurosporine promotes cytochrome *c* release from mitochondria, an early event in apoptosis [17].

We have therefore used a two-stage model of apoptosis in which BE(2)-C cells are primed with butyrate for 18 h (Stage I), and then treated for a further 3 h with staurosporine (Stage II). This model has enabled us to investigate the effect of varying $[Zn^{2+}]_i$ on early and later events in apoptosis of neuroblastoma cells. The subcellular distribution of Zn may provide a clue to its mechanism of action. It is likely that the important pools of Zn in protection against premature apoptosis are the more labile (free or loosely bound) Zn. The bulk of cellular Zn is tightly bound in metalloenzymes and transcription factors and not depleted even in severe Zn deficiency [4, 5, and Refs. within]. These pools were visualized using a membrane-permeant Zn-specific fluorophore Zinquin [5, 18, 19]. In this study we investigated the subcellular distribution of Zn and correlated with effects of varying $[Zn^{2+}]_i$ on the activation of caspase-3 in neuroblastoma cells.

MATERIALS AND METHODS

Materials. Major materials and their suppliers were: A23187, EDTA, EGTA, herring sperm DNA, Nonidet P-40 (NP-40), dithiothreitol, sucrose, Hepes, staurosporine, TPEN, pyrithione (Sigma Chemicals, St. Louis, MO); sodium butyrate (BDH, Poole, England); penicillin/streptomycin, EDTA/trypsin, glutamine, Chaps (ICN, Aurora, OH); gentamicin (David Bull Labs, Melbourne, Vic, Aust); DEVD-AFC (Kamiya Biomedical Co., Tukwila, WA). Zinquin, ethyl-[2-methyl-8-*p*-toluenesulfonamido-6-quinolyloxy]acetate (Dr. A. D. Ward, Department of Chemistry, University of Adelaide, South Australia) [18] was dissolved in DMSO at 5 mM and stored at −20°C in the dark. Staurosporine was stored at −20°C as stock solution (430 μM) in DMSO while TPEN was stored in the same manner at 50 mM. All other reagents were reagent-grade, unless indicated.

Cell cultures. BE(2)-C cells were obtained from ECAAC (#95011817) at passage 17 and cultured in RPMI 1640, Hepes-buffered, pH 7.4 (ICN), supplemented with glutamine (2 mM), penicillin (100 IU/ml), streptomycin (100 μg/ml), gentamicin (160 μg/ml) and 10% fetal bovine serum (Biosciences, Sydney, Aust) in a humidified atmosphere containing 5% CO_2. NIE-115 mouse neuroblastoma cells were a gift of Dr. S. Bolsover (Department of Physiology, University College, London, UK). The cells were allowed to differentiate by exposure to 2% DMSO for 10 days in complete culture medium. Experiments were performed either in 25-cm^2 vented tissue culture flasks or 6-well plates (Sarstedt, Newton, NC). Cells were allowed to attach and grow for 2–3 days in tissue culture flasks prior to exposure to test reagents. For cultures with butyrate, stock solutions (400 mM) in RPMI were made fresh each day and diluted into the cell suspension to give the desired final concentration (in most experiments this was 1 mM).

Induction of apoptosis. Stage I: BE(2)-C cells were primed with 1 mM butyrate for 18 h. Stage II: These cells were then treated for a further 3 h with 1 μM staurosporine. Where Zn status of the cells was increased, $ZnSO_4$ (25 μM) + sodium pyrithione were added at the same time as staurosporine. Where Zn status of cells was decreased, TPEN was added instead of staurosporine.

Assays for apoptosis. Caspase-3 was assayed by cleavage of the fluorogenic substrate zDEVD-AFC (z-asp-glu-val-asp-7-amino-4-methyl-coumarin) [16]. Although DEVD-AFC is a preferential substrate of caspase-3, it has been noted that caspase-7 can also cleave it [18]. Therefore cytosolic enzymatic activity will be referred to by the more general term of DEVD-caspase. Cells (5×10^6–10^7 per flask) were cultured with test reagents, washed 1× with 5 ml of PBS and resuspended in 1 ml of NP-40 lysis buffer (as for DNA fragmentation). After 15 min in lysis buffer at 4°C, insoluble material was pelleted at 15,000*g* and an aliquot of the lysate was tested for protease activity. To each assay tube containing 8 μM of substrate in 1 ml of buffer (50 mM Hepes, 10% sucrose, 10 mM DTT, 0.1% Chaps, pH 7.4), 20 μl of cell lysate was added. After incubation overnight at room temperature, caspase activity was quantified by fluorescence (Excitation wavelength 400 nm, Emission wavelength 505 nm) in a Perkin–Elmer LS50 spectrofluorometer. Optimal amounts of added lysate and duration of assay were taken from linear portions of curves determined in preliminary experiments.

Apoptosis was also confirmed in randomly selected samples by morphological criteria and DNA fragmentation [16]. A minimum of 300 cells from replicate tubes was scored. For morphological assessment, cells were examined by phase contrast microscopy after addition of an equal volume of 0.2% trypan blue in Hank's balanced salt solution (PBS), pH 7.4. Apoptotic cells were distinguishable from normal cells by their nuclear fragmentation, presence of apoptotic bodies, decreased size and sometimes, intense membrane blebbing. Cells with one or more of these properties were scored as positive. In most cases, they excluded trypan blue. In some experiments, acridine orange was added to a final concentration of 10 μM and cells were analyzed by fluorescence microscopy for chromatin segregation.

To assay DNA fragmentation, cells (5×10^6–10^7 in total) were lysed at 4°C in 1 ml of NP-40 lysis buffer (5 mM Tris–HCl, pH 7.5, containing 5 mM EDTA and 0.5% NP-40) and centrifuged at 13,000*g* for 10 min at 4°C. Supernatant fractions containing low-molecular-weight DNA fragments were assayed for DNA by a fluorometric technique [20]. Hoechst dye #33258 was dissolved in deionized water to a concentration of 1 mg/ml and stored at 4°C. Prior to use, 1 μl of dye was added per 10 ml of TE buffer (10 mM Tris–HCl, pH 7.4, containing 1 mM EDTA, and 100 mM NaCl). Aliquots of lysate (20–50 μl) were placed into fluorometer-grade disposable cuvettes (Greiner) and 1 ml of diluted dye solution added. Fluorescence was measured at an excitation wavelength of 356 nm and emission wavelength of 458 nm (slit widths 10 nm) in a Perkin–Elmer fluorescence LS50 spectrophotometer. Herring sperm DNA was used to derive a standard curve (0–8 ng/ml).

Zn supplementation and depletion experiments. $[Zn^{2+}]_i$ was increased in BE(2)-C cells using the Zn ionophore sodium pyrithione [5]. Cells in wells or in coverslips (in complete culture medium) were incubated for the indicated period of time at 37°C with 25 μM exogenous $ZnSO_4$ and indicated concentrations of sodium pyrithione. Cells were then washed four times with PBS to remove extracellular Zn prior to labeling with Zinquin. For calcium loading, cells were treated for the indicated period of time with 0.5 μM calcium ionophore A23187.

$[Zn^{2+}]_i$ was decreased in BE(2)-C cells by treatment with the membrane-permeant Zn(II) chelator TPEN, which binds Zn tightly

and thereby depletes the labile Zn intracellular pool, but not other major intracellular divalent metal ions such Ca and Mg [5]. Cells were incubated for up to 4 h at 37°C with indicated concentrations of TPEN (in complete culture medium).

Fluorescence image analysis. To investigate the subcellular distribution of labile Zn in neuroblastoma cells, we used the membrane-permeant Zn-specific fluorophore Zinquin. Zinquin has a relatively low affinity for Zn (K_d in the nM range) such that it is unable to compete for tightly chelated Zn in metalloenzymes and can only monitor the more labile pools. Cells were grown on poly-L-lysine-coated glass coverslips and incubated with or without $ZnSO_4$ + pyrithione or TPEN for 60 min, as in earlier experiments, before addition of 25 μM Zinquin for a further 30 min at 37°C.

Fluorescence image analysis with Zinquin was performed [5, 19]. Cells were incubated with 25 μM Zinquin in PBS for 30 min at 37°C. For video image analysis, specimens were examined using an Olympus fluorescent microscope, equipped with a UV-B dichroic mirror for low wavelength excitation, and connected to a CCTV video color camera and computer work station. Images were captured and fluorescence was quantified using the Video Pro Image Analysis System (Leading Edge, South Australia).

For greater resolution of the subcellular distribution of Zn in neuroblastoma cells, Zinquin-loaded cells were examined by UV-laser confocal microscopy. Human neuroblastoma cells were examined at the Waite Institute in Adelaide. A Bio-Rad MRC-1000 Laser Scanning Confocal Microscope System, equipped with a UV-Argon laser, was used in combination with a Nikon Diaphot 300 inverted microscope in fluorescence mode with excitation at 363/8 nm and emission at 460LP. Coverslips (25 mm square) containing untreated or treated neuroblastoma cells were inverted onto microscope slides and the edges sealed with nail polish. Images were collected using ×40 water immersion objective lens with NA 1.15. Each image was averaged over 4 scans by Kalman filtering. For the study of rat N1E neuroblastoma cells, the same instrument was used at the Bio-Rad facility in Hemel Hempsted (UK).

Experimental design and data analysis. All experiments were repeated at least three times. The results of typical experiments are described or data were pooled, as indicated in text. Statistical significance was determined by the student *t*-test and is indicated in text or legends to figures.

RESULTS

DEVD-caspase activity. Figure 1A (open circles) shows the modest increase in DEVD-caspase activity when BE(2)-C cells were treated overnight with butyrate. Caspase activity plateaued at 2 mM butyrate with no further increase at concentrations up to 10 mM. A much greater activation of DEVD-caspase occurred when BE(2)-C cells were treated with a combination of butyrate and 1 μM staurosporine (filled circles, Fig. 1A). Synergy with staurosporine was obtained at a range of concentrations of butyrate, but was most evident at lower concentrations (e.g., 1 mM). Thus, 1 mM butyrate alone induced 74.3 ± 12.3 units and 1 μM staurosporine, alone, induced 139.7 ± 28.6 units/10^6 cells of DEVD-caspase, while a combination of the two induced 449 ± 58.0 units.

In the experiment shown in Fig. 1, the total cell population was harvested and assayed for caspase activity. This includes both the adherent (largely viable or preapoptotic) cells and floating (largely apoptotic) cells. Increase in DEVD-caspase activity was found in both populations: attached (open columns, Fig. 1B) and floating (hatched columns, Fig. 1B), consistent with the onset of caspase activation before detachment of the cells from the plates.

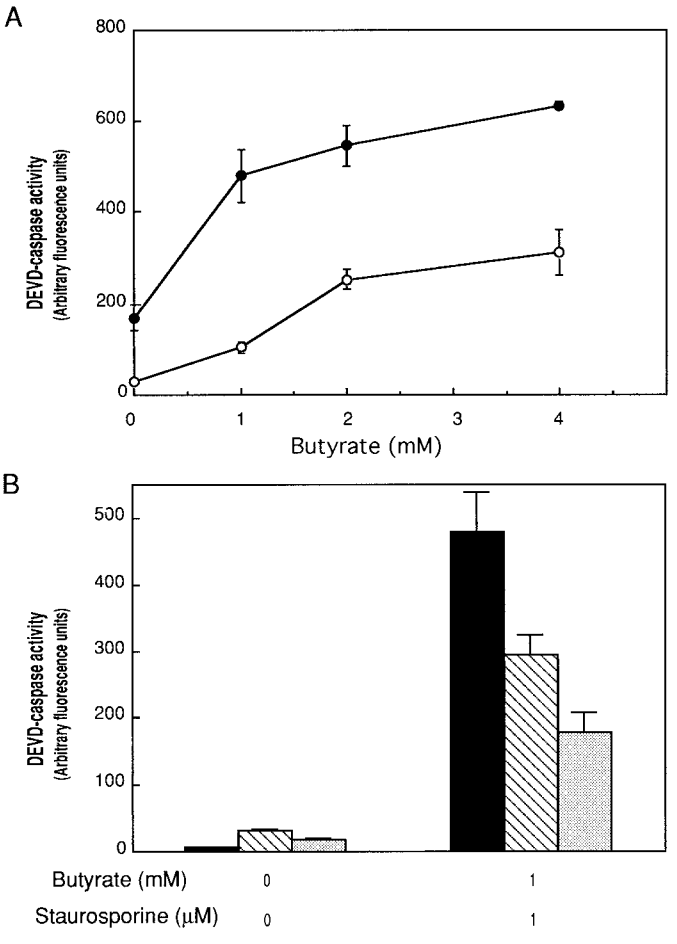

FIG. 1. Interaction between butyrate and staurosporine in activation of DEVD-caspase. (A) Subconfluent monolayers of BE(2)-C cells in wells were treated for 18 h with the indicated concentration of butyrate before further culture for 3 h in the absence (○) or presence (●) of 1 μM staurosporine. Floating cells were then collected and lysed together with adherent cells to yield total cell lysates which were assayed for DEVD-caspase activity. Data are expressed as arbitrary fluorescence units/50 μl of lysate ($2.5–5 \times 10^5$ cells). Bars indicate standard deviations for means of triplicates. A typical experiment is shown. The figure shows synergy between the two toxins, especially at 1 mM butyrate. (B) Treatments were as in A except that in addition to assay of total cell population for DEVD-caspase activity (filled columns), the adherent population (striped columns) and floating population (shaded columns) were assayed individually. Bars indicate standard deviations for means of triplicates. A typical experiment is shown. The figure shows activation of DEVD-caspase in both populations.

Activation of DEVD-caspase was associated with morphological changes of apoptosis. Typical morphological features included presence of one or more intracellular apoptotic bodies, granularity that was often localized to one pole of the cell, exclusion of the vital dye trypan blue, membrane blebbing and, in some

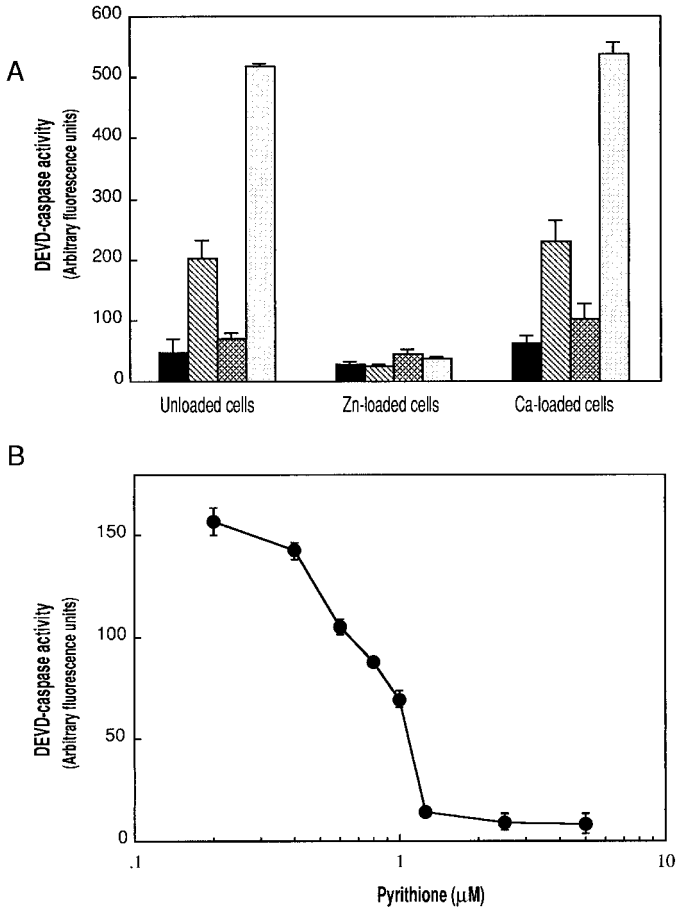

FIG. 2. Effect of increasing $[Zn^{2+}]_i$ on activation of DEVD-caspase. (A) BE(2)-C cells were treated for 18 h without toxin (filled column), with 1 mM butyrate alone (striped columns), with 1 μM staurosporine alone for the final 3 h (hatched columns) or with butyrate plus staurosporine (shaded columns). In the final 3 h, cells were also treated with 25 μM $ZnSO_4$ + 4 μM pyrithione (Zn-loaded cells), with 1 μM A23187 (Ca-loaded cells) or no addition (unloaded cells). Calcium was not added with A23187 because the medium already contains 0.6 mM Ca salts. DEVD-caspase activity represents means of triplicates. The figure shows suppression of DEVD-caspase activation when $[Zn^{2+}]_i$ (but not $[Ca^{2+}]_i$) was increased during the final 3 h. (B) Cells were treated with a combination of butyrate and staurosporine (as in A) and 25 μM $ZnSO_4$ plus varying concentrations of pyrithione were added during the final 3 h. The figure shows concentration-dependent suppression of DEVD-caspase activation. Bars indicate standard deviations. A typical experiment is shown.

cells, reduction in volume. There was also extensive DNA fragmentation as determined by presence of DNA fragments in 13,000*g* supernatants of lysates (not shown).

Increasing intracellular Zn in BE(2)-C cells suppresses DEVD-caspase activation. An increase in $[Zn^{2+}]_i$ after pretreatment of cells with $ZnSO_4$ and Zn ionophore pyrithione strongly suppressed induction of DEVD-caspase activity by the combination of 1 mM butyrate and 1 μM staurosporine (Fig. 2A). By contrast preloading cells with calcium using calcium ionophore A23187 had no effect on induction of apoptosis. 50% inhibition of DEVD-caspase activation occurred with approximately 0.7 μM pyrithione (Fig. 2B).

Decreasing intracellular Zn in BE(2)-C cells increases DEVD-caspase activation. Depletion of $[Zn^{2+}]_i$ by treating cells with the Zn chelator TPEN had a similar effect to staurosporine on the induction of caspase activity. Thus when BE(2)-C cells were primed for 18 h with 1 mM butyrate, the subsequent addition of 25 μM TPEN resulted in a substantial activation of caspase activity (filled squares, Fig. 3A). The increase in caspase activity began about 100 min after the addition of TPEN and increased up to 4 h. Under these conditions 25 μM TPEN alone induced only a little caspase activity (from 7.0 $\pm$ 1.0 to 24.3 $\pm$ 2.9 units). However a higher concentration of TPEN (50 μM) resulted in an 18- to 19-fold increase (127.7 $\pm$ 9.2 units).

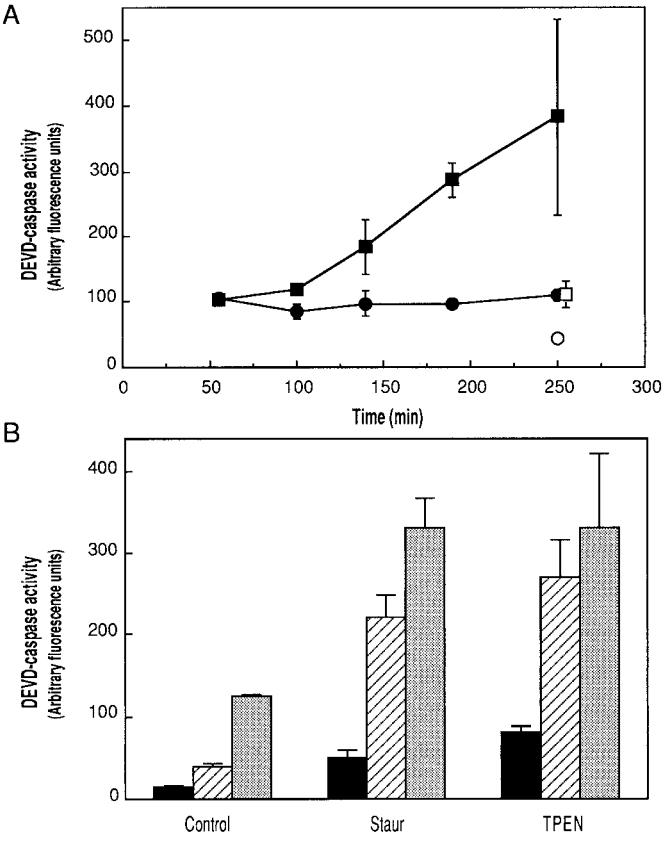

FIG. 3. Interaction between TPEN and butyrate on DEVD-caspase activation. (A) BE(2)-C cells were cultured for 18 h with or without 1 mM butyrate and then for up to a further 250 min in the absence or presence of 25 μM TPEN: Control (○), butyrate alone (●), TPEN alone (□) and butyrate + TPEN (■). DEVD-caspase activity represents means of triplicates; bars indicate standard deviations. Typical experiment is shown. The figure shows strong synergy between butyrate and TPEN, with onset of DEVD-caspase activity after a lag-phase of 100 min. (B) BE(2)-C cells were cultured for 18 h with 0 (filled columns), 1 (striped columns), or 4 (shaded columns) mM butyrate and then for a further 4 h in the absence or presence of 1 μM staurosporine or 25 μM TPEN.

The columns in Fig. 3B show that the synergistic effect of TPEN was very similar to that caused by staurosporine. In agreement with this, a combination of TPEN and staurosporine had an additive rather than synergistic effect on DEVD-caspase activity.

Distribution of labile Zn in neuroblastoma cells. To better understand the mechanism of action of Zn on neuronal apoptosis, $[Zn^{2+}]_i$ was visualized and quantified in neuroblastoma cells using the Zn-specific fluorophore Zinquin. Figures 4A–4C shows pseudo-colored images of the levels of Zn in BE(2)-C cells obtained by conventional fluorescence microscopy. TPEN-treated neuroblastoma cells (Fig. 4A) had minimal fluorescence compared with the basal fluorescence in untreated cells (Fig. 4B). A marked increase in fluorescence was seen when cells were treated with $ZnSO_4$ + pyrithione (Fig. 4C). Figures 4D and 4E showed the strong cytoplasmic Zinquin fluorescence in the Zn-loaded cells: fluorescence had a starry-sky appearance.

Next, we studied Zn distribution in neuroblastoma cells possessing a more differentiated morphology; for this, we used the mouse neuroblastoma cell line NIE-115 that is induced to form axon-like neurites when cultured in the presence of 2% DMSO. After 10 days in culture with DMSO, large proportion of these cells had neurites. Zinquin fluorescence was investigated without further addition of exogenous Zn. Typical cells are shown in Fig. 4F. There was little fluorescence in the cell body except for the Golgi region (upper panel of Fig. 4F), while there was strong fluorescence (green–red) in the neurite with an apparent cytoskeletal distribution (lower panel of Fig. 4F). At the foot of the neurite, there was also intense fluorescence, which may correspond to Zn-rich presynaptic vesicles.

DISCUSSION

The main finding of this study is that Zn significantly modulates an early event in apoptosis of neuroblastoma cells. Increasing $[Zn^{2+}]_i$ in a neuroblastoma cell line suppressed toxin-induced activation of DEVD-caspase, a key effector of neuronal apoptosis. Decreasing $[Zn^{2+}]_i$ rendered the cells much more susceptible to activation of this enzyme. Fluorescence images of Zinquin-loaded neuroblastoma cells revealed a paucity of nuclear labile Zn. Although Zn is expected to be abundant in the transcription factors and nucleic acid synthesizing enzymes, this Zn is tightly bound and unlikely to be available for Zinquin binding. It is unlikely that Zinquin is excluded from the nuclear compartment, since Zinquin labels Zn in other membrane bound organelles [19]. Zinquin fluorescence at the neurite terminal may represent a vesicular pool of Zn analogous to the Zn-rich secretory vesicles in the presynaptic terminals of certain neurons [8]. However it is not possible at this stage to determine actual free Zn concentrations from the fluorescence intensities. The apparent localization of Zinquin-stainable Zn in the cytoskeleton of neuroblastoma cells is consistent with the pronounced effect of Zn deprivation on the stability of the microtubular cytoskeleton. In marginally Zn-deficient rats, brain Zn concentration was decreased accompanied by microtubular destabilization and defective tubulin polymerization, which were retarded at an early stage, and were normalized following addition of Zn to the brain extracts [9, 21]. It is interesting that the microtubules are disrupted not only in Zn deficiency, but also in apoptosis where microtubule rearrangement is a common early feature.

The microtubular cytoskeleton is also disrupted in AD and infusion of colchicine (microtubule toxin) into the hippocampi of rats resulted in similar alterations to those in AD [22]. Intracellular neurofibrillary tangles, a hallmark of AD, may represent a cytoskeletal disturbance in a subset of neurons undergoing apoptosis. Since both Zn ions and tau (membrane associated protein) bind to tubulin and stabilize microtubules [21, 23, 24], tau phosphorylation and Zn deficiency may have similar functional effects on the cytoskeleton at the neuropathological level. Zn promotes noncovalent interaction between S100b and tau, resulting in total inhibition of tau phosphorylation by Ca^{2+}/calmodulin-dependent protein kinase II [25]. Apart from directly stabilizing the cytoskeleton, Zn may also be protective by limiting access of aluminum, a neurotoxin that binds to and disrupts the neuronal cytoskeleton [26].

We propose a two-stage model for activation of DEVD-caspase by neurotoxin and Zn deficiency. In the first stage, toxins such as butyrate induce expression of a pro-apoptotic protein, which triggers changes in the neuronal cytoskeleton that result in the formation of neurofibrillary tangles. In the second stage, a Zn-deficient environment (achieved by depleting tubulin-bound Zn) destabilizes the cytoskeleton and thereby renders the neuron more susceptible to cytoskeletal damage. Disruption of the cytoskeleton can initiate a cascade of events involving the proteolytic conversion of pro-caspases to their active forms, cleavage of critical proteins and cellular fragmentation into apoptotic bodies.

We believe that the findings of this study have important implications for AD, where apoptosis is thought to be the predominant mechanism of the excessive cell death [1, 2] and Zn homeostasis is altered. The beneficial role of Zn [27–31] or its deleterious effects [32–34] are unresolved. An age-associated tissue deficiency of Zn in the brains of AD patients may be caused by sequestration of Zn within amyloid plaques [33] and displacement of Zn by other metals such as aluminum and lead [26]. This study identifies $[Zn^{2+}]_i$ as a critical factor in determining susceptibility of neuronal-like cells to toxin-induced activation of a major cell-death inducing protease. This supports the

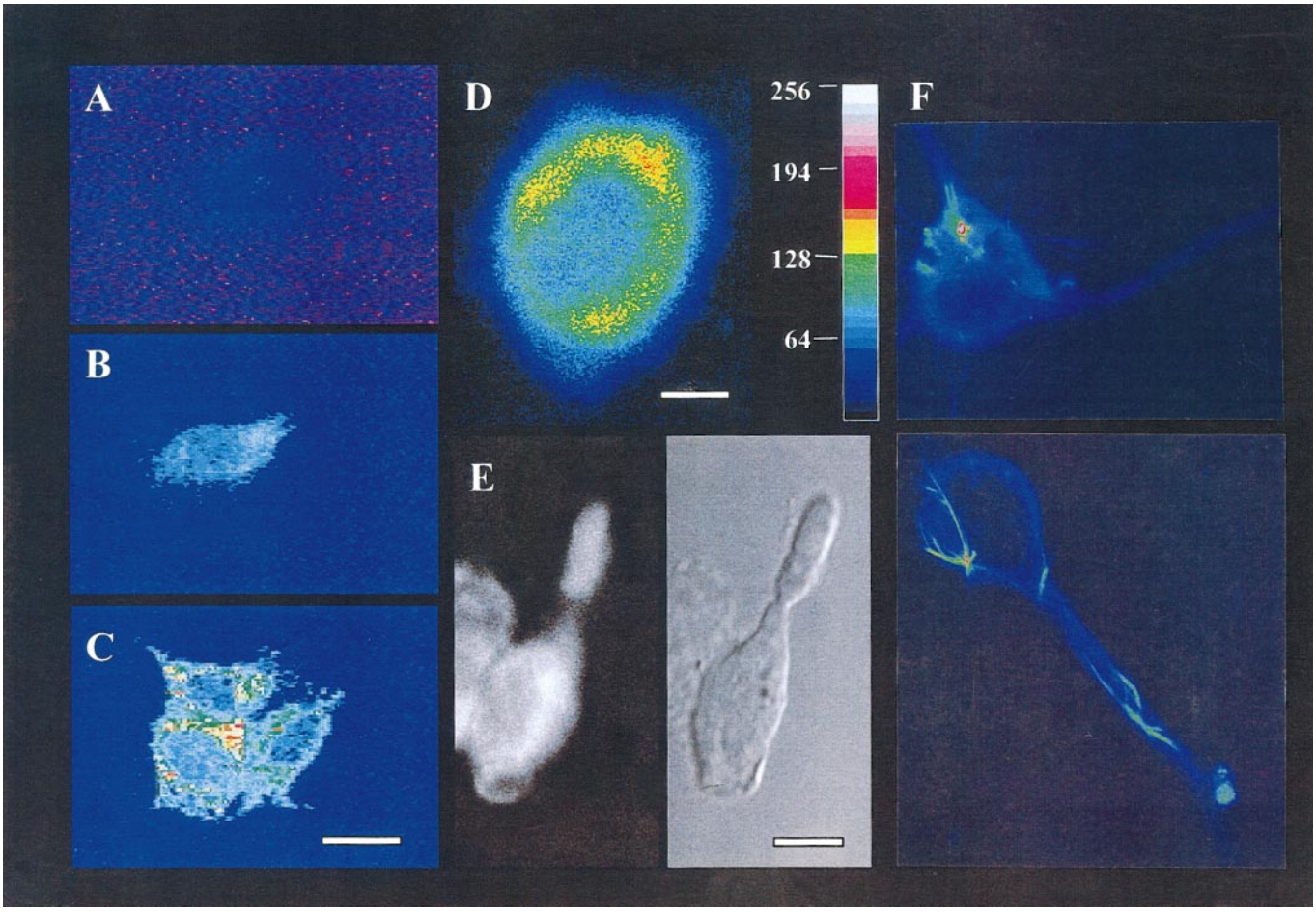

FIG. 4. Zn-dependent Zinquin fluorescence studies. (A–C) UV-fluorescence microscopy. Pseudo-colored images of Zn-dependent Zinquin fluorescence in BE(2)-C cells. Cells were pretreated (as indicated below) for 60 min before addition of Zinquin. Typical cells are shown. Scale bar in C indicates 12 μm. (A) 25 μM TPEN (Zn-deficient). (B) No pretreatment (basal Zn level). (C) 25 μM ZnSO4 + 4 μM pyrithione (Zn-loaded). (D–F) UV-laser confocal microscopy. (D, E) Confocal image of Zn-loaded BE(2)-C cells showing cytoplasmic fluorescence. D is a pseudo-colored image, while E show real fluorescence. Scale bar in D indicates 5 μm and in E indicates 10 μm. (F) Pseudo-colored images of DMSO-differentiated NIE-115 cells, showing the basal fluorescence pattern. Upper panel show strong fluorescence in the Golgi region, lower panel shows cytoskeletal pattern of fluorescence and fluorescence labeling at the foot of the neurite which may represent presynaptic vesicles. Scale bar for F is shown in E and indicates 8 μm.

view of Potocnik and colleagues [35] who have reported a modest improvement in symptoms following Zn supplementation. Zn supplementation may be effective if commenced early to maintain adequate intracellular Zn levels, thus delaying the progress of the disease. There is however a greater need to understand the mechanism of apoptosis in neuronal cells and the role of Zn deficiency in AD.

ACKNOWLEDGMENTS

We thank Dr. S. Bolsover (Department of Physiology, University College, London, UK) for supplying the NIE-115 neuroblastoma cells. We are also grateful to the Bio-Rad Workshop in Hemel Hempsted, UK, and Dr. P. Kolesik (Waite Institute, University of Adelaide) for UV laser confocal microscopy studies. We acknowledge Dr. A. Bush (Massachusetts General Hospital) for helpful discussions. This work was supported in part by grants from the National Health and Medical Research Committee, the Australian Research Council, and the University of Adelaide.

REFERENCES

1. Smale, G., Nichols, N. R., Brady, D. R., Finch, C. E., and Horton, W. E. (1995) *Exp. Neurol.* **133,** 225–230.
2. Anderson, A. J., Su, J. H., and Cotman, C. W. J. (1996) *Neuroscience* **16,** 1710–1719.
3. Kerr, J. F. R., Searle, J., Harmon, B. V., and Bishop, C. J. (1987) Apoptosis in Perspectives of Mammalian Cell Death, Oxford Univ. Press, Oxford.
4. Zalewski, P. D., and Forbes, I. J. (1993) Programmed Cell Death: The Cellular and Molecular Biology of Apoptosis, Harwood Academic, Melbourne.
5. Zalewski, P. D., Forbes, I. J., and Betts, W. H., (1993) *Biochem. J.* **296,** 403–408.
6. Golub, M. S., Keen, C. L., Gershwin, M. E., and Hendricks, A. G. (1995) *J. Nutr.* **125**(Suppl.), 2263S–2271S.

7. Vallee, B. L., and Falchuk, K. H. (1993) *Physiol. Rev.* **73,** 79–118.
8. Frederickson, C. J. (1989) *Int. Rev. Neurobiol.* **31,** 145–238.
9. Oteiza, P. I., Cuellar, S. B., Lonnerdal, Hurley, L. S., and Keen, C. L. (1990) *Teratology* **41,** 97–104.
10. Takahashi, A., Alnemri, E. S., and Lazebnik, Y. A. (1996) *Proc. Natl. Acad. Sci. USA* **93,** 8395–8400.
11. Kuida, K., Zheng, T. S., Na, S., Kuan, C. Y., Yang, D., Karasuyama, H., Rakic, P., and Flavell, R. A. (1996) *Nature* **384,** 368–372.
12. Talanian, R. V., Quinlan, C., Trautz, S., Hackett, M. C., Mankovich, J. A., Banach, D., Ghayur, T., Brady, K. D., and Wong, W. W. (1997) *J. Biol. Chem.* **272,** 9677–9682.
13. Perry, D. K., Smyth, M. J., Stennicke, H. R., Salvesen, G. S., Duriez, P., Poirier, G. G., and Hannun, Y. A. (1997) *J. Biol. Chem.* **272,** 18530–18533.
14. Liu, X., Kim, C. N., Pohl, J., and Wang, X. (1996) *J. Biol. Chem.* **271,** 13371–13376.
15. Nuydens, R., Heers, C., Chadarevian, A., De Jong, M., Nuyens, R., Cornelissen, F., and Geerts, H. (1995) *Brain Res.* **688,** 86–94.
16. Medina, V., Edmonds, B., Young, G. P., James, R., Appleton, S., and Zalewski, P. D. (1997) *Cancer Res.* **57,** 3697–3707.
17. Kluck, R. M., Bossy-Wetzel, E., Green, D. R., and Newmeyer, D. D. (1997) *Science* **275,** 1132–1136.
18. Mahadevan, I., Kimber, M. C., Lincoln, S. F., Tiekink, E. R. T., Ward, A. D., Betts, W. H., Forbes, I. J., and Zalewski, P. D. (1996) *Aust. J. Chem.* **49,** 561–568.
19. Zalewski, P. D., Millard, S. H., Forbes, I. J., Kapaniris, O., Slavotinek, A., and Betts, W. H. (1994) *J. Histochem. Cytochem.* **42,** 877–884.
20. Teare, J. M., Islam, R., Flanagan, R., Gallagher, S., Davies, M. G., and Grabau, C. (1997) *Biotechniques* **22,** 1170–1174.
21. Nickolson, V. J., and Veldstra, H. (1972) *FEBS Lett.* **23,** 309–313.
22. Nakagawa, Y., Nakamura, S., Kase, Y., Noguchi, T., and Ishihara, T. (1987) *Brain Res.* **408,** 57–64.
23. Yankner, B. A. (1996) *Neuron* **1,** 921–932.
24. Serrano, L., Dominguez, J. E., and Avila, J. (1988) *Anal. Biochem.* **172,** 210–218.
25. Baudier, J., and Cole, R. D. (1988) *J. Biol. Chem.* **263,** 5876–5883.
26. Shea, T. B., Wheeler, E., and Jung, C. (1997) *Mol. Chem. Neuropathol.* **32,** 17–39.
27. Constantinidis, J. (1991) *Med. Hypotheses* **35,** 319–323.
28. Licastro, F., Davis, L. J., Mocchegiani, E., and Fabris, N. (1996) *Biol. Trace Elem. Res.* **51,** 55–62.
29. Basun, H., Forssell, L. G., Wetterberg, L., and Winblad, B. (1991) *J. Neural Transm. Park. Dis. Dement.* **3,** 231–258.
30. Prasad, A. S., Fitzgerald, J. T., Hess, J. W., Kaplan, J., Pelen, F., and Dardenne, M. (1993) *Nutrition* **9,** 218–224.
31. Sandstead, H. H. (1991) *Am. J. Dis. Child.* **145,** 853–859.
32. Danscher, G., Jensen, K. B., Frederickson, C. J., Kemp, K., Andreasen, A., Juhl, S., Stoltenberg, M., and Ravid, R. J. (1997) *Neurosci. Methods* **76,** 53–59.
33. Bush, A. I., Pettingell, W. H., Multhaup, G., Paradis, M., Vonsattel, J. P., Gusella, J. F., Beyreuther, K., Masters, C. L., and Tanzi, R. E. (1994) *Science* **265,** 1464–1467.
34. Loo, D. T., Copani, A., Pike, C. J., Whittemore, E. R., Walencewicz, A. J., and Cotman, C. W. (1993) *Proc. Natl. Acad. Sci. USA* **90,** 7951–7955.
35. Potocnik, F. C., van Rensburg, S. J., Park, C., Taljaard, J. J., and Emsley, R. A. (1997) *S. Afr. Med. J.* **87,** 1116–1119.